ICSV14
Cairns • Australia
9-12 July, 2007

14th International Congress on Sound & Vibration

ACOUSTICALLY CONTROLLED ROTATIONS OF A DISK IN FREE FIELD

Arturo O. Santillán[1], Karen Volke-Sepúlveda[2] and Ricardo R. Boullosa[1]

[1] Centro de Ciencias Aplicadas y Desarrollo Tecnológico, Universidad Nacional Autónoma de México, Circuito Exterior s/n, Cd. Universitaria, A. P. 70-186, 02510 México D. F., México
[2] Instituto de Física, Universidad Nacional Autónoma de México, A. P. 20-364, 01000 México D. F., México
arturo.orozco@ccadet.unam.mx

Abstract

In general, forces are caused on objects when sound waves interact with their surfaces. Based on this phenomenon, acoustical levitation is a technique in which stationary sound fields are used to trap small samples, liquid or solid, compensating the action of gravity. Rotations of suspended objects in acoustic levitation devices are common, which are due mainly to asymmetries of the samples and sometimes to instabilities of the system. This fact turns out to be disadvantageous for applications where a precise control of the sample position is desired. The general objective of this work has been to study the extent to which it is possible to transfer angular momentum from a sound field to matter, and to control the rotations of an object. An original contribution of the work is that the acoustic fields have been produced in free space, i.e., without the need of a cavity, which gives the advantage of free access to the sample. We present an analysis of the properties of acoustic fields analogous to optical vortices; by using these kinds of sound fields, we show experimentally the generation of rotations in a solid disk produced by acoustic waves. In addition, by generating acoustic vortices of the first and second orders, we demonstrate that the direction of rotation is consistent with the corresponding helicity; we also analyse the differences of the angular momentum transfer between both cases. On this basis, we conclude that this mechanism can be used to achieve rotational control of acoustically levitated objects.

1. INTRODUCTION

The study of acoustic forces had a first significant impulse approximately three decades ago, when they were considered as potential tools for positioning objects in spaceships. In recent years, with the development of transducers capable of generating acoustic waves of high amplitude, a renewed interest in acoustic forces has arisen since they can be used to manipulate and process materials in a non-invasive way, avoiding contact with tools or the use of containers. Small objects of any density, solids or liquids, with no special electric or magnetic properties, can be levitated by a standing sound field [1].

The use of acoustic forces is particularly advantageous in the manipulation of small samples. For instance, although it is easy to trap objects with tweezers or micro-tools, to release them again is not simple; the objects or part of the materials often remain adhered to the manipulation instruments or containers. In addition, the forces produced by acoustic waves are distributed over the whole surface of the sample; there are no "point forces" that could damage the structure of fragile objects.

Even though samples can be acoustically levitated for long periods, it is not rare to observe rotations of suspended objects, particularly in non-spherical solids. This fact turns out to be disadvantageous for several applications, such as precise manipulation of objects, crystal growth, and observation of samples through microscopes. In other cases, however, a controlled rotation of the levitated objects may be desirable, for instance, in the evaporation of drops from liquid-solid suspensions. The rotations of acoustically levitated objects can either saturate to a constant angular velocity or evolve into chaotic movements, giving rise in the latter case to an escape of the object from the acoustic trap. Therefore, the need of precise rotational control in acoustic levitation devices becomes a main subject of interest.

A way to produce rotations of objects by sound waves has been reported by using a rectangular cavity with two sides of the same length [2-6]. When two degenerated modes are simultaneously excited, but with a phase difference between them, a torque is exerted on an object in the cavity. The torque has the maximum value at a phase difference of ± 90 degrees, and the direction of the induced rotations depends on the sign of the phase difference. The disadvantage of this technique to control the rotations of levitated samples is the need of the rectangular cavity, which prevents free access to the sample.

As a starting point, we intended to establish the acoustic analogous to the so-called optical vortices. In 1992, it was demonstrated by Allen and co-workers that optical vortices possess a well-defined orbital angular momentum (OAM) [7], which is different from the spin angular momentum associated with circular polarization. Years later, it was proved that both spin and OAM can be transferred to optically trapped microparticles [8]. Whereas spin angular momentum causes a torque on a trapped particle about its own axis, OAM causes the particle to rotate about the beam axis [9].

In this paper we demonstrate that acoustical vortices can indeed be generated, and by this means it is possible to transfer angular momentum to matter from acoustical waves in free field conditions. Moreover, two different sound fields have been studied theoretically and have been experimentally achieved; one is similar to a first order vortex and the other one to a second order vortex. We compare the differences between the two sound fields, and we analyse the torques generated on a disk in each case.

2. THEORY

2.1. Acoustic Vortices

In optics, three basic propagation modes can be identified among light beams with circular cylindrical symmetry, namely, the cosine modes whose complex amplitude has the form $\Psi = u(\rho,z)\cos(l\varphi)$, the sine modes with $\Psi = u(\rho,z)\sin(l\varphi)$, and the rotating modes or optical vortices with $\Psi = u(\rho,z)\exp(\pm il\varphi)$. In all these cases, (ρ,φ,z) represent the usual cylindrical coordinates, and $u(\rho,z)$ is an arbitrary complex function. One way of generating optical vortices is by means of an appropriated superposition of cosine and sine modes as follows

$$\Psi(\mathbf{r}) = u(\rho, z)\{\cos(l\varphi) \pm i\sin(l\varphi)\}. \quad (1)$$

This is depicted schematically in Figure 1 for the case l=1 and with $u(\rho,z)$ corresponding to the so called Laguerre-Gauss beams [7]. While the phase of the sine and cosine modes have only the values 0 and π, the superposition results in a linear variation from 0 to 2π around the mode circumference, which gives rise to a rotation of the vortex phase as the wave field propagates. The sign in Eq. (1) determines the direction of rotation, so that the vortex may have either positive helicity (plus sign) or negative helicity (minus sign).

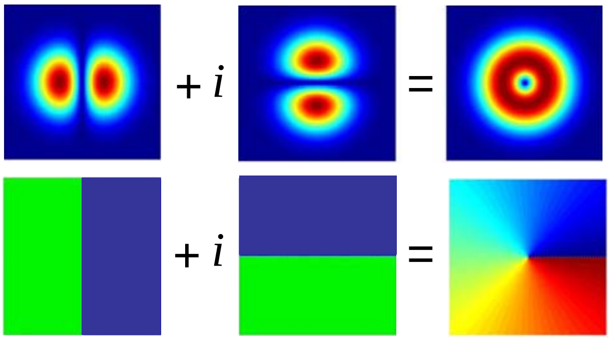

Figure 1. Generation of a first order optical vortex from the superposition of a cosine and a sine modes out of phase by $\pi/2$. The first row represents the intensity, where blue is the minimum and red is the maximum values. The second row is the phase, where blue represents zero, green represents π and red represents 2π.

With these ideas in mind, we generated a kind of first order acoustic vortex in free field with four equal simple sources. They should be placed equidistantly around a circumference of radius a, and they should be driven with a phase difference of $\pm\pi/2$ with respect to the adjacent sources. Thus, the complex amplitude $p(\boldsymbol{r})$ of the total sound field generated by the four sources at the observation position $\boldsymbol{r}$ can be described by

$$p(\mathbf{r}) = \sum_{n=1}^{N} \frac{A}{r_n} \exp\{\text{-}i\, kr_n\} \exp\{\pm i(n-1)\pi/2\}\,. \tag{2}$$

Here r_n is the distance from the n-th simple source to a point in the space, A/r_n is the pressure amplitude of the wave generated by the n-th source with A a real constant, and N=4. In a similar way, a kind of second order acoustic vortex can be produced by means of eight simple sources equidistantly distributed around a circumference. In this case, Eq. (2) is also appropriate to describe the acoustic field, but with N=8; in general, for producing an acoustical vortex of order l, N=4l independent sources will be required.

Considered the simple sources located in the xy planes of a reference system with the centre of the circumference at the origin. Under the conditions $x^2 + y^2 << a^2 + z^2$ and $|kax|$, $|kay|$ << $\sqrt{a^2+z^2}$, where (x, y) denote the transverse variables in any horizontal plane, the wave field of Eq. (2) along the vertical axis (z) for N=4 can be approximated as

$$p(\mathbf{r}) \approx 2iA \frac{ka}{a^2 + z^2} \sqrt{x^2 + y^2} \exp\{\text{-}i\, k(a^2 + z^2)^{1/2}\} \exp\{\pm i\phi\}\,. \tag{3}$$

The term $\exp(\pm i\phi)$ appears explicitly here, which is characteristic of a first order vortex. Under the same conditions, we can get a similar equation for the sound field generated with the eight simple sources, and in this case a term of the form $\exp(\pm i2\phi)$ is obtained, corresponding to a second order vortex.

The graphs of the acoustic intensity in the plane z = 5 cm are illustrated in Figure 2 for the two studied sound fields; here a = 18.5 cm and λ = 26.4 cm. We can observe the energy circulation around the origin, which is a fingerprint of a vortex. Since the fluid density variations are proportional to the sound pressure, the linear momentum of the fluid is in turn proportional to the sound intensity. Therefore, according to Figure 2, a disk centred at the origin (see Fig. 3) is expected to rotate in the same direction as the sound intensity.

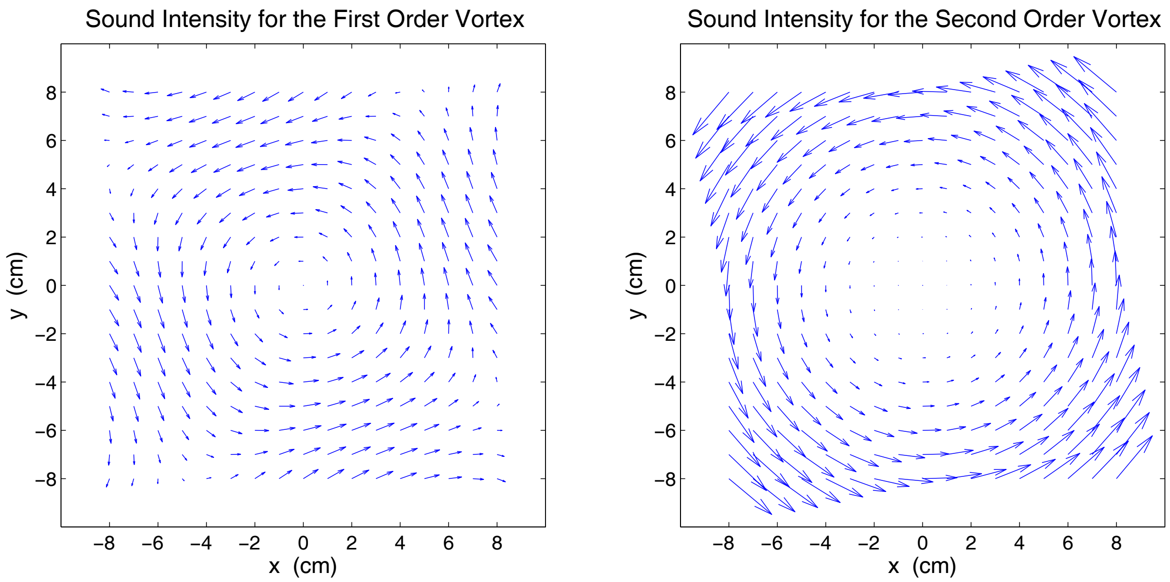

Figure 2. Theoretical sound intensity on the plane z = 5 cm corresponding to the two studied vortices.

It should be observed that the contribution to the total torque on the disk from the acoustic field is expected to be small around the origin; this is a consequence of the fact that the amplitude of the acoustic pressure is zero at that point for both acoustic fields. Therefore, the contribution to the total torque will be more significant in outer regions. As a result, one can expect that the bigger the diameter of the disk, the larger the torque. It is worth mentioning, that this is also a characteristic of optical vortices, which exhibit a dark core on-axis surrounded by light, giving rise to a transverse intensity pattern that resembles a doughnut of light (see Figure 1, last column on the right); the larger the order of the vortex, the larger the diameter of the dark spot at the centre.

The graphs of the two sound fields at a given time (snapshots) are shown in Figure 4. One can see that there is a continuous phase cycle of 2π radians around a circumference for the sound field produced with four sources, and two cycles of 2π for the acoustic wave generated with eight sources. These are characteristics of first order and second order vortices, respectively. There is a significant difference between the two acoustic fields; for the first order vortex, the magnitude of the particle velocity has a maximum value in the origin, whereas there is a particle velocity node at that point for the second order vortex.

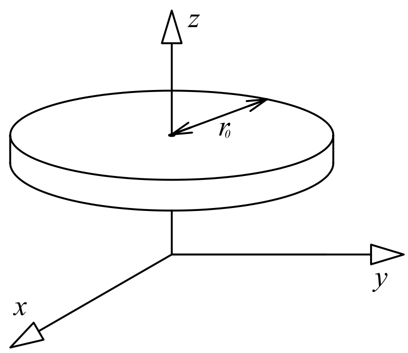

Figure 3. Reference frame used for the calculation of the acoustic torque exerted on a disk or radius r_0.

2.2. Acoustic Torque

Consider an object with surface S immersed in a sound field with complex amplitude p and angular frequency ω. The time average of the component of the acoustic torque $\boldsymbol{\tau}$ parallel to a unit vector **a** exerted on the object is given by [5]

$$< \tau > \; = \; < \boldsymbol{\tau} \cdot \boldsymbol{a} > \; = \; -\frac{\delta_v}{4} \oint_S \mathrm{Re}\left\{ (\boldsymbol{n} \times \nabla)^2 \, \frac{p}{\omega} (1+i) \, [(\boldsymbol{a} \times \boldsymbol{r}) \cdot \boldsymbol{u}]^* \right\} ds \;, \quad (4)$$

where, $\mathbf{r} = (x, y, z)$ is the position vector from the origin to a point on S, δ_υ is the viscous penetration depth, $\mathbf{u}$ is the particle velocity assuming zero viscosity (equal to $i\nabla p/\rho\omega$), and b^* represents the complex conjugate of the variable b.

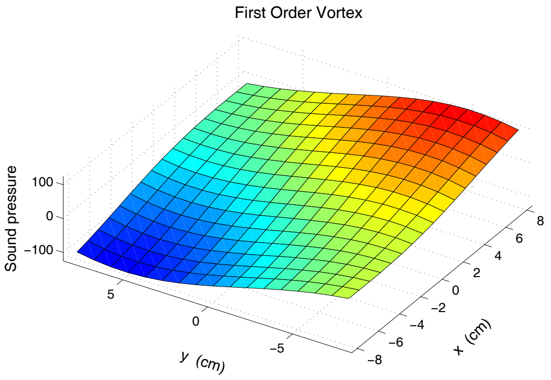

Figure 4. Theoretical distribution of the sound pressure on the plane z = 5 cm at a given time (snapshot) for each of the two studied acoustic vortices.

For the case depicted in Figure 3, the acoustic torque in the z direction exerted on the disk of negligible thickness and parallel to the xy plane can be obtained from Eq. (4) as

$$< \tau_z > = -\frac{\delta_v}{4\omega} \oint_S \mathrm{Re}\left\{ \left(\frac{\partial^2}{\partial x^2} + \frac{\partial^2}{\partial y^2} \right) p \; (1+i) \left[x u_y - y u_x \right]^* \right\} ds \, . \tag{5}$$

Notice that if the sound pressure is independent of z, $(\partial^2/\partial x^2+\partial^2/\partial y^2)\, p = \nabla^2 p = -k^2 p$ and the acoustic torque becomes proportional to the sound intensity.

It should be observed, according to Figure 2, that even for positions on the disk that do not satisfy the conditions $x^2 + y^2 << a^2 + z^2$ and $|kax|$, $|kay|$ << $\sqrt{a^2 + z^2}$, the total exerted torque within the sound field is expected to be very large, sometimes even higher than the case where these conditions are fulfilled. In fact, to get a large acoustic torque, we used in our experiment a disk with a radius that is not very small compared to a nor to λ.

3. EXPERIMENT

The experimental setup is illustrated in Figure 4. Eight drivers (for horn loudspeakers) are distributed around a circumference of radius a = 18.5 cm. For generating the first order acoustic vortex, only four of them are activated, the ones on the axes of the coordinate system; whereas the eight drivers are used to generate the second order vortex. Each driver is connected to an independent channel of an audio amplifier (two channels per amplifier). In turn, the four amplifiers are fed by using eight channels of an external sound card controlled with a PC. The signals to be reproduced, including the allotted phase differences, are generated by means of a computing program (Matlab 7.0).

To have a precise control of the phase differences and the pressure levels, each reproduce chain was individually characterized. Any undesired difference in the level and phase produced by each driver was compensated when the signals were created. In addition, the sign of the topological charge was set to cover the $2\pi l$–phase cycles in either clockwise or counterclockwise directions. For the characterization process we used a two-channel FFT signal analyser; the sound field was measured with an omni-directional precision microphone placed 4 cm from the baffle on the *z* axis.

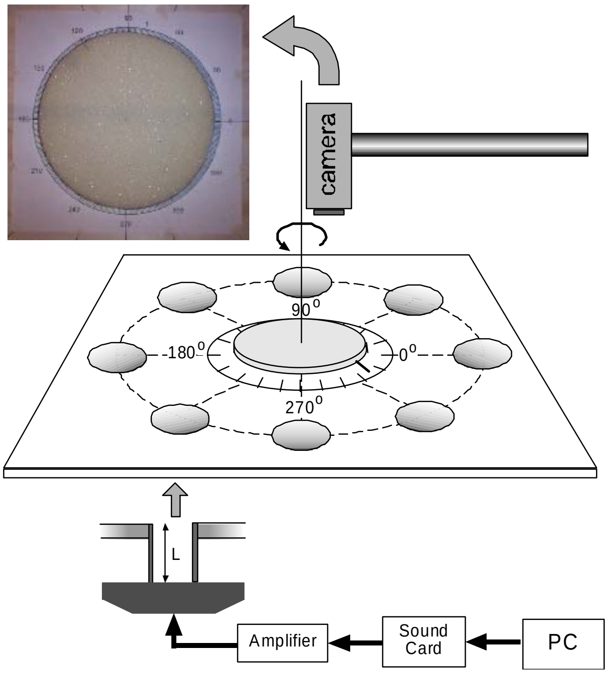

Figure 5. Experimental setup for the transfer of angular momentum from an acoustical vortex to a hanging disk in a torsion pendulum.

The optimum performance of the whole device took place at the resonant frequency of the drivers. A tube was placed at the output of each driver, connecting it to the baffle; in this way, the resonant frequency was modified by the length *L* of the tubes. The resonance was shifted up to 1300 Hz with *L* = 6 cm, but the device can be operated from 1100 to 2500 Hz with a reasonable good performance.

For measuring the acoustic torque, we implemented a twist pendulum with an optical fibber of high linear stiffness and a hanging disk of radius r_o=8.1 cm, which was made of acrylic (1.68 mm thick) and with both sides covered with a rubber foam layer (3.3 mm thick). We covered both sides of the disk with robber foam because we observed that the acoustic absorption of the surface of the disk has a significant role in the transfer of angular momentum from the sound field, as has been reported by Schroeder [6]. Among several alternatives of rubber foam, we chose one with open pore and the highest acoustic absorption. Underneath the disk, on the baffle, we placed a 360º protractor with resolution of 1°, and we fixed a pin at the edge of the disk to make the angle measurements (inset picture on the upper left corner of Figure 5). All the experiments were realized with the device inside an anechoic chamber.

When the sound field was generated, the disk rotated an angle θ to a new equilibrium position, where the acoustic torque generated by the vortex was exactly balanced by the opposite torque exerted by the torsion of the optical fibber. The torque in the torsion pendulum is given by $\tau = -\kappa\theta$, where κ is the rotational stiffness equal to

$$\kappa = 4\pi^2 I_{disk} / T^2 . \qquad (6)$$

Here $I_{disk} = \pi r_o^4 \sigma/2$ is the moment of inertia of the disk of mass M = 43.21 g; σ is the mass surface density of the disk, which was calculated to be 0.21 g/cm^2; and T = 52.66 s is the oscillation period of the pendulum. As a result, κ = 20.18 dn·cm/rad was found.

4. RESULTS AND DISCUSSION

The disk was initially placed at a height of 0.9 cm from the baffle. However, instabilities were observed in the disk inside the first order vortex at the higher sound pressure levels of the considered interval. The disk swung, and this movement affected its rotational motion. This prevents us from determining the correct angle of rotation. In addition, when the disk moved in a stable way, for the lower sound levels used, the angles of rotation were small, less than 20º. With the second order vortex, however, instabilities did not show up, and the torque was obtained. The problem of the instabilities with the first order vortex disappeared when the disk was lifted at a higher distance over the baffle; in this way, the determination of the torque for that vortex was possible with the disk at a height of 4.9 cm.

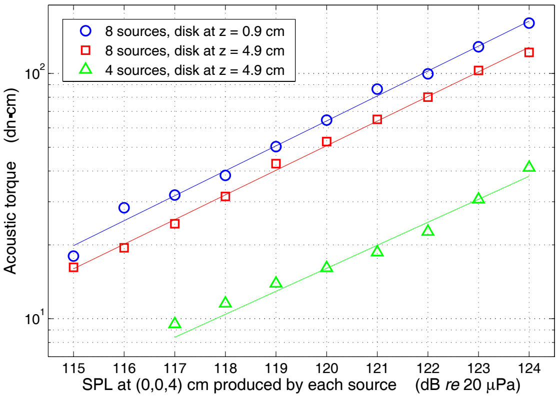

Figure 6. Acoustic torque exerted on a disk with a radius of 8.1 cm for different values of the sound pressure.

The measured acoustic torques are shown in Figure 6. The sound pressure levels in the *x* axis of the graph were measured, without the disk, at 4 cm from the baffle and with only one driver operating. It can be observed that the experimental data can be fitted quite well to a straight line in a logarithmic plot. For the two curves corresponding to the second order vortex, the values of the slope are 2.034 and 2.007 for the disk at 0.9 cm and 4.9 cm, respectively. These values coincide with the fact that the acoustic torque depends on the square of the sound pressure amplitude, according to Eq. (4). For the case of the first order vortex, however, the slope is equal to 1.88. This slope, smaller than the expected value of two, may be explained by the fact that the magnitude of the particle velocity for the first order vortex is larger around the *z* axis; therefore, acoustic energy is efficiently absorbed by the rubber foam around the centre of the disk, but the contribution to the total torque is very small in that zone. According to Figure 6, the second order vortex was more efficient at transfering angular momentum to the disk. In addition, by comparing the two curves for the second order vortex, corresponding to the two different heights of the disk, the torque was is slightly larger for the disk closer to the baffle.

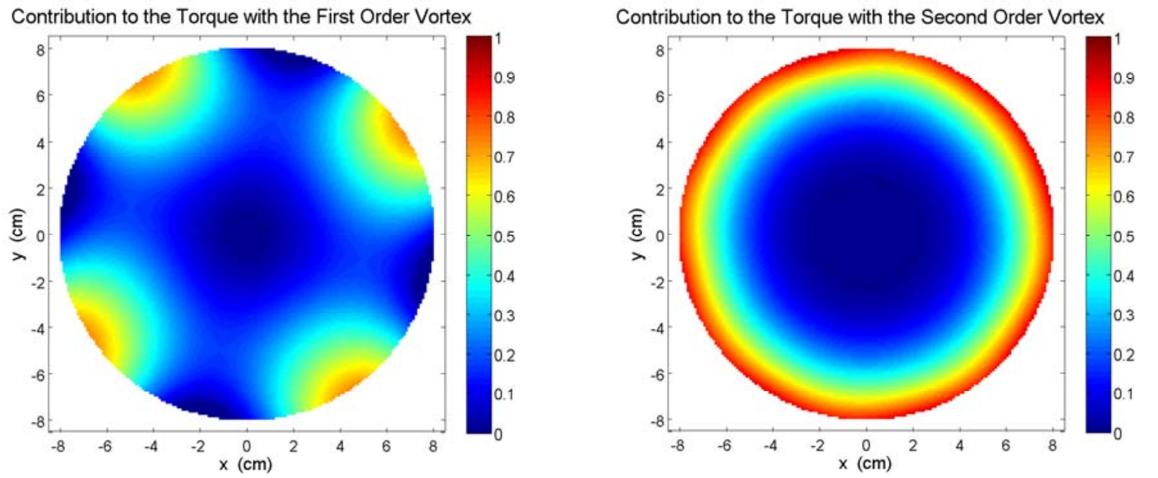

Figure 7. Theoretical distributions of the acoustic torque per unit surface of the disk for the two studied sound fields. The height was 5 cm from the baffle.

The difference in the torque applied on the disk, between the first and second order vortices, can be understood by analysing the contributions to the total torque from the different parts of its surface. The distributions of the torque per unit surface of the disk for the two studied sound fields are shown in Figure 7. They were obtained according to the integrand of Eq. (5). The results of these graphs give only a good qualitative approximation to the actual situation, since the effects of diffraction were not taken into account in our calculations, and the acoustic absorption is not described by Eq. (5). We can see that around the central region of the disk, the contribution to the total torque is very small; in fact, the transfer of angular momentum is even less efficient in that region for the second order vortex. This is consistent with the observations made above on the graphs of the sound intensity. However, as the distance from the origin increases, the acoustic field is more uniform for the second order vortex. The contribution to the total torque for this sound field seems to be independent of the azimuthal angle along the surface of the disk, and increases with the distance to the origin. On the other hand, the torque per unit area of the first order vortex has an azimuthal dependence for values of r larger than approximately 4 cm, equal to 0.15 times λ, where there are also four regions with a very small contribution to the total torque.

5. CONCLUSIONS

In this work, we have demonstrated for the first time, to our knowledge, that angular momentum can be transferred from a sound field to matter under free field conditions, without the need of a resonant cavity. The wave fields generated for such a task are the acoustical analogous of the so called optical vortices; we studied, theoretically and experimentally, acoustical vortices of first and second orders. An absorbent disk suspended from a torsion pendulum was used to quantify the acoustical torque. The magnitude of the acoustic torque depends linearly on the acoustical energy, as expected, but it also depends on the vortex charge, the wavelength, and the size of the disk. In particular, it was found that the second order acoustic vortex produces a higher torque than the first order one, on an object, when it is larger than approximately 0.15 times the wavelength. In additon, the second order vortex generates more stable conditions of the rotation of the disk. Future work will aim to perform a more detailed characterization of the system in order to optimize the acoustical torque. And finally the implementation of the system in acoustic levitation devices. This will give the advantage of having rotational control while keeping free access to the suspended sample. For this purpose, ultrasound will be used, which allows the reduction of the size of the system, and at the same time avoids the annoyance of audible sound.

ACKNOWLEDGEMENT

Authors would like to thank DGAPA-UNAM for the financial support, project INI114407-3.

REFERENCES

[1] W. J. Xie, C. D. Cao, Y. J. Lü, Z. Y. Hong and B. Wei, "Acoustic method for levitation of small living animals", Applied Physics Letters 89, 214102, 2006.

[2] T. G. Wang, H. Kanber, and I. Rudnick, "First-order torques and solid-body spinning velocities in intense sound fields", Phys. Rev. Lett. 38, 128-131, 1977.

[3] T. G. Wang, H. Kanber, and E. E. Olli, "Fourth-order acoustic torque in intense sound fields", J. Acoust. Soc. Am. 63, 1332 -1335, 1978.

[4] A. Biswas, E. W. Leung, and E. H. Trinh, "Rotation of ultrasonically levitated glycerol drops", J. Acoust. Soc. Am. 90, 1502-1507, 1991.

[5] F. H. Busse and T. G. Wang, "Torque generated by orthogonal acoustic waves—Theory", J. Acoust. Soc. Am. 69, 1634-1639, 1981.

[6] M. R. Schroeder, "Circularly polarized acoustic fields: the number theory connection", Acustica 75, 94-98, 1991.

[7] L. Allen, M. W. Beijersbergen, R. J. C. Spreeuw, and J. P. Woerdman, "Orbital angular momentum of light and the transformation of Laguerre-Gaussian laser modes," *Physical Review A* **45**, 8185-8189 (1992).

[8] M. E. J. Friese, J. Enger, H. Rubinsztein-Dunlop, and N. R. Heckenberg, "Optical angular-momentum transfer to trapped absorbing particles," *Physical Review A* **54**, 1593-1596 (1996).

[9] V. Garces-Chavez et. al., "Observation of the transfer of the local angular momentum density of a multi-ringed light beam to an optically trapped particle," *Physical Review Letters* **91**, 093602 (2003).